LO-09-002 (RP-1311)

Solar Gain through Windows with Shading Devices: Simulation Versus Measurement

Nathan A. Kotey
Student Member ASHRAE

John L. Wright, PhD, PEng
Member ASHRAE

Charles S. Barnaby
Member ASHRAE

Michael R. Collins, PhD, PEng
Associate Member ASHRAE

This paper is based on findings resulting from ASHRAE Research Project RP-1311.

ABSTRACT

Shading devices offer a cost saving strategy in dynamically controlling solar gain through windows. As such, there is an ongoing effort to accurately quantify the thermal performance of shading devices. In the present study, solar gain through various shading devices attached to a conventional double glazed window was measured using the National Solar Test Facility (NSTF) solar simulator and solar calorimeter. The shading devices include two venetian blinds, a roller blind, a pleated drape and an insect screen. More specifically, the solar heat gain coefficient (SHGC) and the solar transmittance, τ_{sys}, of each system were measured; and the interior attenuation coefficient (IAC) was calculated from the SHGC measurements. Furthermore, SHGC, τ_{sys} and IAC were calculated for the same experimental conditions using models developed for building energy simulation and performance rating. The calculations agreed very well with the measurements.

INTRODUCTION

In buildings with significant cooling loads solar gain is especially troublesome because it is generally the largest and most variable heat gain the building will experience. As a result, window shading attachments that can be used for solar control are drawing attention and a renewed effort is being made to develop models for devices such as venetian blinds, drapes, roller blinds and insect screens (e.g., van Dijk et al. 2002, Rosenfeld et al. 2000, Pfrommer et al. 1996, ISO 2004, Yahoda and Wright 2004, 2005, Kotey et al. 2009a, b, c, d). Window shading attachments also offer the benefit of being operable and many devices such as venetian blinds and roller blinds can be automated. Thus, shading attachments can be used efficiently to admit solar energy when and where heating, and possibly lighting, is required but reject it otherwise.

Computer simulation offers a means to evaluate the energy saving performance of shading attachments, their potential to reduce peak cooling loads and the effectiveness of various control strategies. However, until recently, the detailed simulation of shading attachments was routinely neglected. Research is currently geared toward the modeling of shading attachments for building energy simulation but these models are also useful for design and rating. Such an effort has led to the development of various models for complex fenestrations systems (i.e., systems containing glazing and shading layers) in building energy simulation and performance rating software like ParaSol v3.0 (Hellstrom et al. 2007), EnergyPlus 2007, WINDOW 6.1/THERM 6.1 (Mitchell et al. 2006) and WIS (van Dijk et al. 2002). However, some of the models in the aforementioned software are either limited in their capabilities or not general enough to handle certain combinations of glazing/shading layers.

To expand the scope of shading attachment modeling to include more common devices, an ASHRAE Research Project 1311-RP (Wright et al. 2009, Barnaby et al. 2009) was undertaken. This research project has led to the development of fenestration shading models designated ASHWAT (ASHRAE Window ATtachment). ASHWAT models are currently implemented in an enhanced version of the ASHRAE Loads Toolkit (Barnaby et al. 2004, Pedersen et al. 2001).

The ASHWAT models were developed for four specific types of window attachments: drapes, venetian blinds, roller blinds and insect screens. There are significant differences

Nathan A. Kotey is a PhD student, **John L. Wright** is a professor, and **Michael R. Collins** is an associate professor in the Department of Mechanical and Mechatronics Engineering, University of Waterloo, Waterloo, Ontario, Canada. **Charles S. Barnaby** is the vice-president of research at Wrightsoft Corporation, Lexington, MA.

between these categories and any one of these categories represents a very large variety of products. In order to retain generality and practicality while striking a balance between complexity and computational speed a simplified approach was taken regarding the way in which radiation interacts with a shading layer. Two points are worth mentioning.

- Shading layers are characterized by making the assumption that each layer, whether homogeneous or not, can be represented by an equivalent homogenous layer that is assigned spatially-averaged "effective" optical properties. This approach has been used in a number of studies (e.g., Parmelee and Aubele 1952, Farber et al. 1963, Rheault and Bilgen 1989, Pfrommer et al. 1996, Rosenfeld et al. 2000, Yahoda and Wright 2004, 2005) and has been shown to provide accurate characterization of venetian blinds (e.g., Huang et al. 2006, Wright et al. 2008, Kotey et al. 2008a).
- Some portion of the incident solar radiation passes undisturbed through openings in a shading layer and the remaining portion is intercepted by the structure of the layer. The structure may consist of yarn, slats, or some other material. The portion of the intercepted radiation that is not absorbed will be scattered and will leave the layer as an apparent reflection or transmission. These scattered components are assumed to be uniformly diffuse. In addition, a shading layer will generally transmit longwave radiation (i.e., it is diathermanous), by virtue of its openness, and effective longwave properties are assigned accordingly.

Using effective optical properties and a beam/diffuse split of solar radiation at each layer, the framework used to represent multi-layer systems provides virtually unlimited freedom to consider different types of shading layers. This framework also delivers the computational speed needed in the context of building energy simulation (Wright et al. 2009, Barnaby et al 2009).

To evaluate and validate the ASHWAT models, solar gain through various shading devices attached to a conventional double glazed (CDG) window was measured using the National Solar Test Facility (NSTF) solar simulator and solar calorimeter. Performance parameters including solar heat gain coefficient (SHGC), interior attenuation coefficient (IAC) and solar transmittance, τ_{sys}, were obtained for a conventional double glazed (CDG) window as well as various CDG/shading layer combinations. The shading devices include dark and light coloured venetian blinds, a medium coloured roller blind, a medium coloured drape, and a dark coloured fibreglass insect screen. Performance parameters were also obtained for the same conditions using the ASHRAE Toolkit simulations that incorporate ASHWAT models.

PERFORMANCE PARAMETERS

When solar radiation is incident on a fenestration system a portion will be directly transmitted to the indoor space while other portions are absorbed by the individual layers, some of which is redirected to the indoor space by heat transfer. For a given fenestration system, the solar gain is characterised by the SHGC which is the ratio of the solar gain to the solar irradiance. In a multi-layer fenestration system consisting of n layers, the SHGC can be expressed as

$$SHGC = \tau_{sys} + \sum_{i=1}^{n} N_i \cdot A_i \quad (1)$$

where τ_{sys} is the solar transmittance; A_i and N_i are respectively the absorbed portion of incident solar radiation and the inward flowing fraction of the absorbed solar radiation in the i^{th} layer.

A shading attachment will generally reduce solar gain and this effect may be conveniently represented by the IAC.

$$IAC = \frac{SHGC_{cfs}}{SHGC_g} \quad (2)$$

where $SHGC_{cfs}$ and $SHGC_g$ are SHGC values for the shaded and unshaded glazing system, respectively. Historically, IAC has been presented as a constant depending only on glazing and shade properties (e.g., ASHRAE 2005). However, IAC also depends on solar incidence angle, especially for shades having non-uniform geometry (e.g., venetian blinds, pleated drapes). The IAC is an important parameter since it is required to determine solar gain using cooling load calculation procedures such as ASHRAE's Radiant Time Series (RTS) method.

MEASUREMENTS

Facility

The experiments were performed using the NSTF solar simulator and solar calorimeter. This measurement facility is capable of measuring the SHGC and the U-factor of a full scale window with or without shading layers. Figure 1 is a schematic of the measurement apparatus. Measurements can be carried out under a variety of imposed weather conditions using a solar simulator arc-lamp source and a solar calorimeter positioned in a large environmentally-controlled chamber. The lamp, in combination with an optical reflector system, provides a uniform irradiance over the test area with a spectral irradiance distribution that approximates the ASTM AM1.5 solar spectrum (ASTM E891-87 1987). The intensity of the incident flux at the test section can be adjusted from 100 to 1100 W/m^2 (32 to 350 Btu/ft^2·h). The angle of incidence can be varied from 0° to 30° above the horizontal.

The calorimeter consists of an outer and an inner cell with an absorber plate within the inner cell. The outer cell is designed to provide a stable temperature environment for the inner cell while the absorber plate adds or removes heat from the inner cell. The amount of heat entering or leaving the inner cell can be accurately measured using the heat exchanger loop connected to the absorber plate.

The environmental chamber can be maintained at temperatures ranging from -20 to +50°C (-4 to 122°F). The

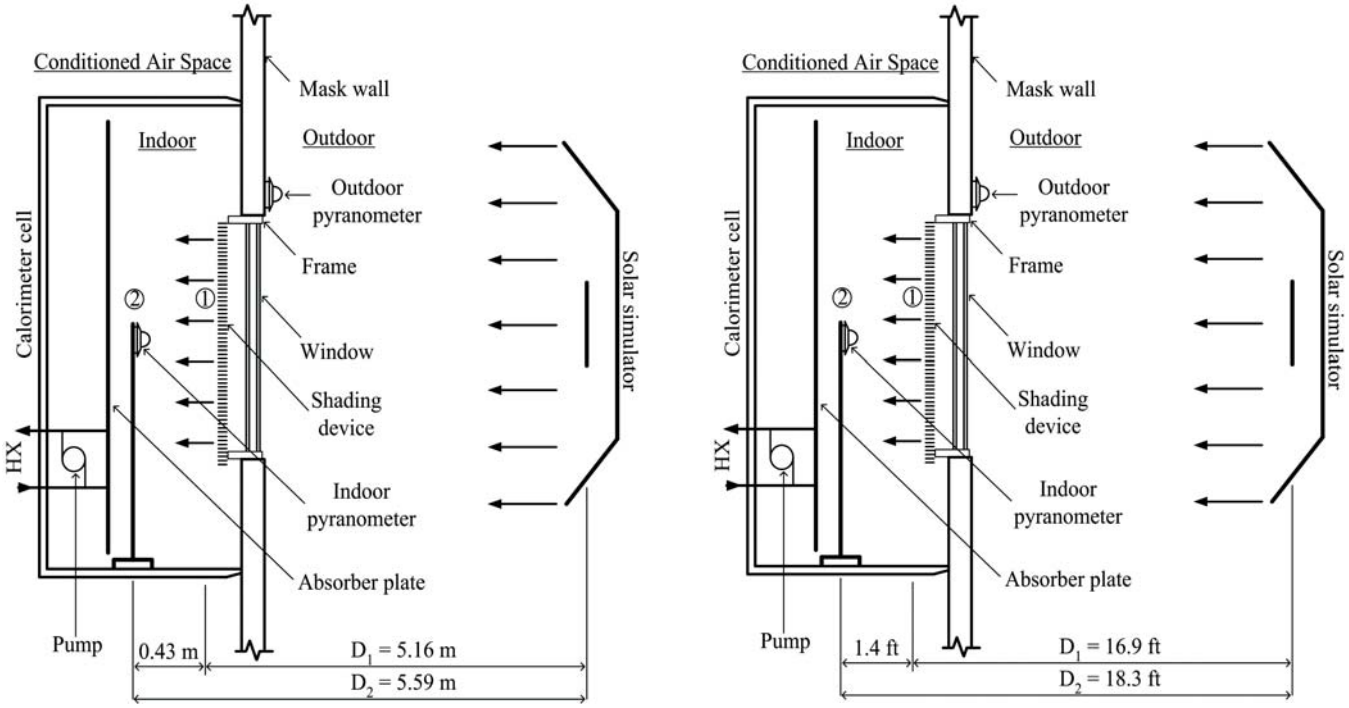

Figure 1 *Schematic of measurement apparatus: (a) SI units and (b) I-P units.*

temperature set point in the chamber can be maintained within ±1°C (±1.8°F). A variable speed fan incorporated in the chamber's air-circulating system provides wind with speeds ranging from 0.5 to 4.0 m/s (1.6 to 13 ft/s). The wind direction is normal to the plane of the test sample. A detailed description of the theory and the operating principles of the NSTF solar simulator and solar calorimeter can be found in several references (e.g., Harrison and Dubrous 1990, CANMET 1993, van Wonderen 1995).

Procedure

Measurements were taken using the window in combination with various shading devices. The test method is similar to the method prescribed by CSA A440.2-98 (1998).

First, the window was mounted in the mask wall of the calorimeter test cell. The test cell was then placed inside the environmental chamber with the mask wall facing the solar simulator. Test conditions including solar irradiance, G_{inc}, indoor air temperature, T_{in}, and outdoor air temperature, T_{out} were maintained at steady state while the net energy transfer through the window, Q_{net}, was measured. During each test a still air condition was maintained on the indoor side of the window with a small fan mounted near the top of the inner cell to eliminate stratification. Wind, with a steady speed of 2.9 m/s (9.5 ft/s) perpendicular to the window, was mechanically maintained at the outdoor side of the window. The experiment was carried out with solar irradiance at normal incidence. In subsequent experiments, shading devices were attached to the window and the test was repeated. Table 1 shows a summary of glazing/shading system test combinations and associated test conditions.

Estimating the Surface Convection Heat Transfer Coefficients

Previous experiments under similar convection conditions using a Calibration Test Standard (CTS) gave a total (i.e., including both convection and radiation) indoor surface heat transfer coefficient of $h_{tot,in}$ = 9.6 ±1.9 W/m^2·K (1.7 ±0.3 Btu/ft^2·h·°F) and a total outdoor surface coefficient of $h_{tot,out}$ = 16.5 ±5.3 W/m^2·K (2.9 ±0.9 Btu/ft^2·h·°F) (van Wonderen 1995). Given the indoor surface temperature of the CTS (glass), $T_{g,in}$, and the indoor mean radiant temperature, T_{in} (assumed equal to the air temperature), the indoor radiative heat transfer coefficient, $h_{r,in}$, was estimated by treating the window as a small object in a large enclosure. See Equation 3.

$$h_{r,\,in} = \varepsilon_{glass}\sigma(T_{g,\,in}^2 + T_{in}^2)(T_{g,\,in} + T_{in}) \qquad (3)$$

Table 1. Summary of Glazing/Shading Layer Test Combinations and Associated Test Conditions

Sample Description	Location	G_{inc}, W (Btu/hr)	T_{in}, °C (°F)	T_{out}, °C (°F)
CDG window	NA	306 (1044.1)	20.3 (68.5)	19.7 (67.5)
CDG window + black insect screen	Outdoor	512 (1746.9)	20.4 (68.7)	19.9 (67.8)
CDG window + beige pleated drape (100% fullness)	Indoor	374 (1276.1)	20.6 (69.1)	19.8 (67.6)
CDG window + white venetian blind (closed)	Indoor	299 (1020.2)	19.9 (67.8)	19.9 (67.8)
CDG window + white venetian blind (fully opened)	Indoor	254 (866.6)	20.3 (68.5)	20.2 (68.4)
CDG window + white venetian blind (slat angle = 30^0)	Indoor	305 (1040.7)	21.4 (70.5)	20.8 (69.4)
CDG window + white venetian blind (slat angle = 60^0)	Indoor	281 (958.8)	20.6 (69.1)	20.8 (69.4)
CDG window + grey roller blind	Indoor	295 (1006.5)	21.1 (70.0)	20.8 (69.4)
CDG window + black venetian blind (slat angle = 60^0)	Indoor	223 (760.9)	20.8 (69.4)	20.7 (69.3)

where σ is the Stefan-Boltzmann constant and $\varepsilon_{glass} = 0.84$ is the emissivity of glass. The outdoor radiative heat transfer coefficient, $h_{r,out}$, was estimated in a similar manner.

$$h_{r,\,out} = \varepsilon_{glass}\sigma(T_{g,\,out}^2 + T_{out}^2)(T_{g,\,out} + T_{out}) \quad (4)$$

In this case $T_{g,out}$ and T_{out} are respectively the outdoor surface temperature of the CTS glazing and the outdoor mean radiant temperature (again assumed equal to the air temperature). The temperatures obtained during calibration, i.e., T_{in}, $T_{g,in}$, $T_{g,out}$ and T_{out}, are listed in Table 2. Since the surface coefficient, h_{tot}, is of sum of the radiative and the convective components, the values of $h_{c,in}$ and $h_{c,out}$were estimated using Equations 5 and 6

$$h_{c,\,in} = h_{tot,\,in} - h_{r,\,in} \quad (5)$$

$$h_{c,\,out} = h_{tot,\,out} - h_{r,\,out} \quad (6)$$

giving $h_{c,in}$ = 4.6 W/m^2·K (0.8 Btu/ft^2·h·°F) and $h_{c,out}$ = 10.0 W/m^2·K (1.8 Btu/ft^2·h·°F). These convective heat transfer coefficients were needed as input data for the ASHWAT simulation models.

Test Samples

The window used in this study was a pre-fabricated insulated glazing unit (IGU) mounted in a fixed wooden frame. The shading devices that were attached to the window include commercially available insect screen, pleated drape, venetian blinds and roller blind. The distance between glazing/shading layers is given in Table 3. The window and shading devices are described below and detail is also provided in Table 4.

Insulated Glazing Unit and Frame. The air-filled IGU consists of two 3 mm (0.12 in.) layers of clear glass separated by a commercially produced edge seal comprising foam spacer and butyl sealant to give an air gap of 12.7 mm (0.5 in.). The IGU was mounted in a wooden frame (unpainted pine). The frame design enabled easy attachment of shading devices. Figure 2 shows a cross-section of the window and the mounting details in the mask wall of the solar calorimeter.

Table 2. Temperatures Obtained during CTS Experiments of van Wonderen (1995)

T_{in}, °C (°F)	$T_{g,in}$, °C (°F)	T_{out}, °C (°F)	$T_{g,out}$, °C (°F)
21.2 (70.2)	26.7(80.1)	47.5 (117.5)	50.7 (123.3)

Table 3. Distance between Glazing/Shading Layers

Glazing/Shading Layers	L, mm (in.)
Two glazings	12.7 (0.5)
Glazing and insect screen	20.0 (0.8)
Glazing and venetian blind	42.0 (1.7)
Glazing and roller blind	72.0 (2.8)
Glazing and pleated drape	100.0 (3.9)

The projected area of the window was divided into three sub-areas: the centre-glass area, A_{cg}, the edge-glass area, A_{eg}, and the frame area, A_{fr}. The centre-glass area is defined as that part of the view area more than 63.5 mm (2.5 in.) from the sight line (e.g., CSA A440.2-98 1998, ASHRAE 2005) and the edge-glass area consists of the remaining part of the view area. The frame area consists of the portion lying outside the sight line. Figure 2 also shows the sub-areas of the window. The total projected window area, A_w, is the sum of A_{cg}, A_{eg} and A_{fr} while the total glass area (view area), A_g, is sum of A_{cg} and A_{eg}. The dimensions of A_w were 1665 × 1665 mm (65.6 × 65.6 in.) and the dimensions of A_g were 1590 × 1590 mm (62.6 × 62.6 in.).

Insect Screen. The insect screen selected for this study was a fibreglass cloth, black screen. It had 18 × 16 mesh per square inch and a strand diameter of approximately 0.38 mm (0.015 in.) giving it an openness factor of 0.58. During testing, the insect screen was attached to the frame at the outdoor side of the window with the aid of staples. This arrangement sealed the screen at its perimeter. The distance between the outdoor glazing and the screen was approximately 20 mm (0.8 in.).

Table 4. Description of Window and Shading Devices

Sample	Description
Window	IGU, two 3 mm (0.12 in.) clear glass, 12.7 mm (0.50 in.) air gap, butyl rubber spacer, wood frame, 1665 × 1665 mm (65.6 × 65.6 in.) total window area, 1590 × 1590 mm (62.6 × 62.6 in) total glass area
Insect screen	Black, fiberglass, 60% openness, 18 x 16 mesh per square inch, 0.38 mm (0.015 in.) strand diameter
Pleated drape	Beige fabric, closed weave, 100% fullness
Venetian blind (1)	White, curved, metallic slats, 24.5 mm (1.0 in.) slat width, 19.1 mm (0.75 in.) slat spacing, 2.3 mm (0.09 in.) slat crown
Venetian blind (2)	Black, curved, metallic slats, 24.5 mm (1.0 in.) slat width, 19.1 mm (0.75 in.) slat spacing, 2.3 mm (0.09 in.) slat crown
Roller blind	Grey, vinyl mesh, 10% openness, 0.80 mm (0.03 in.) thick

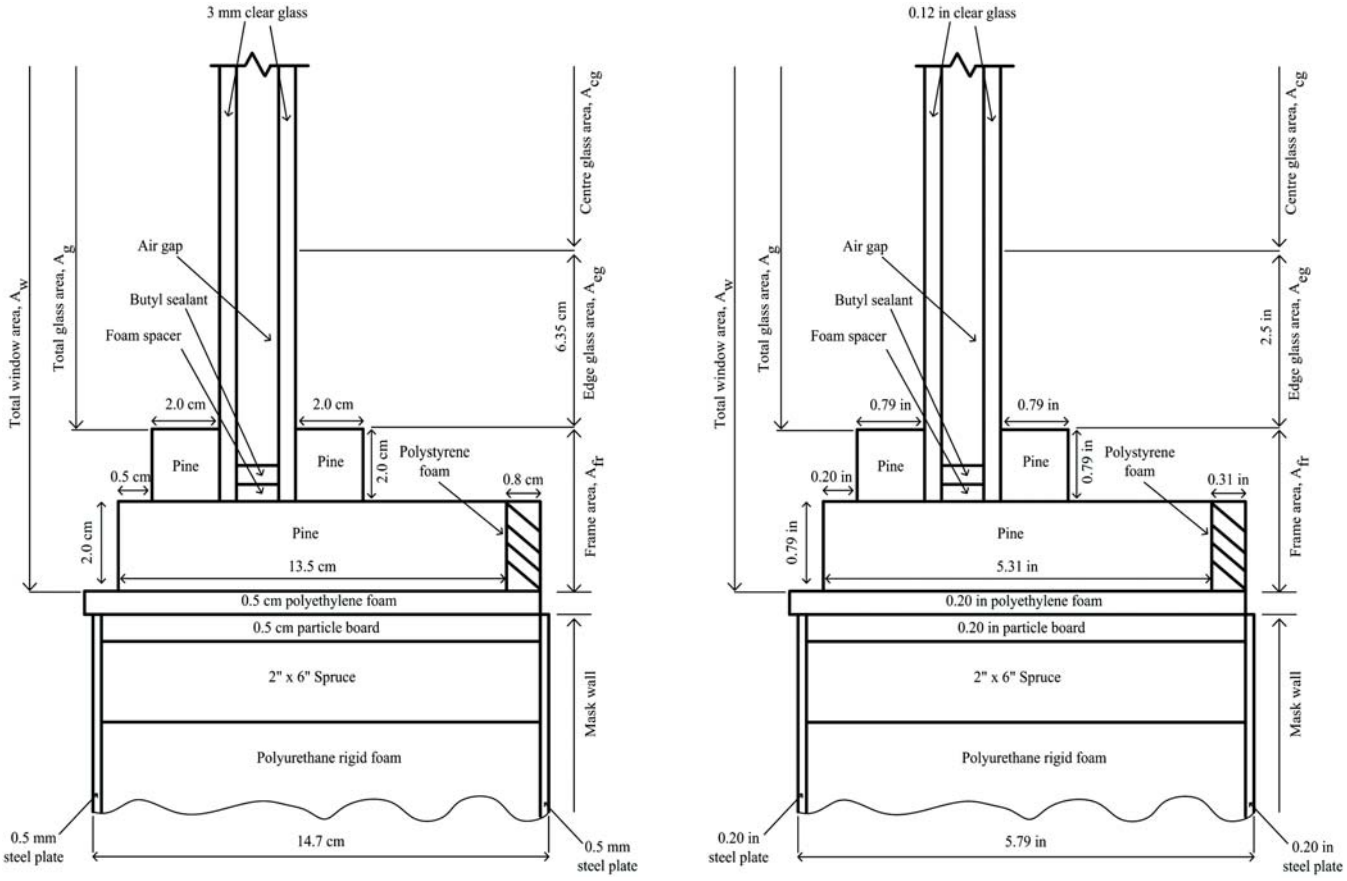

Figure 2 *Cross-sectional details of window and mask wall mounting: (a) SI units and (b) I-P units.*

Pleated Drape. A beige coloured, closed weave, pleated drape was selected for testing. To obtain 100% fullness the width of the flat fabric was twice the width of the pleated drape. During testing the drape was mounted at the indoor side of the window with the aid of a curtain rod affixed to the frame. The drape covered the entire width of the window when installed in its pleated configuration. The distance between convex pleat surfaces and the window was about 100 mm (3.9 in.). The pleats were regularly arranged with an approximately sinusoidal cross-section. There were approximately ten pleats with an average pleat width and spacing of 127 and 178 mm (5.0 and 7.0 in.), respectively.

Venetian Blinds. Two venetian blinds were selected for testing. One blind had black painted slats and the other had white painted slats. The slats were metallic and curved with 24.5 mm (1.0 in.) slat width, 19.1 mm (0.75 in.) slat spacing and 2.3 mm (0.09 in.) slat crown. These blinds were mounted at the indoor side of the window. In the fully opened position, the distance between the indoor glazing and the tip of the slats was approximately 42 mm (1.7 in.). Both blinds were tested at a slat angle of 60°. The white blind was tested with slats at three additional positions, fully opened (slat angle = 0°), closed (slat angle = 75°) and partially opened (slat angle = 30°). At each slat angle other than zero, the convex slat surfaces faced the outdoor side and the slat tips nearer the outdoor side were oriented downward.

Roller Blind. An open weave, grey, vinyl roller blind was selected for testing. The thickness of the roller blind material was 0.80 mm (0.03 in.) and its openness factor was $A_o = 0.10$. The roller blind was mounted on the indoor side of the window at a distance of 72 mm (2.8 in.) from the indoor glazing and the edges were left unsealed so that room air could circulate between the blind and glazing.

Solar and Longwave Properties of Glazing and Shading Materials

Table 5 lists the normal incidence solar properties and longwave properties of the glazing and shading materials. The solar properties include beam-total transmittance, τ_{bt}, beam-total reflectance, ρ_{bt}, beam-diffuse transmittance, τ_{bd}, and beam-beam transmittance, τ_{bb}. The longwave properties are the emissivity, ε, and the longwave transmittance, τ_{LW}. Each material is symmetrical with respect to solar and longwave properties so there is no need to distinguish between front and back properties. To obtain the solar properties, spectral measurements were taken at normal incidence using a commercially available spectrophotometer (Kotey et al. 2009a, b and c). The shading materials are generally not spectrally selective except for variation in the visible wavelength band corresponding to the colour of the material. The solar properties were calculated using the 50-point selected ordinate method as described in ASTM E903-96 (1996). The longwave properties were measured with a commercially available infrared reflectometer (Kotey et al. 2008b). The measured longwave properties of the shading materials are included in Table 5. However, the measured longwave properties of drapery fabric, roller blind material and the insect screen were not needed because empirical relations included in the ASHWAT models (Kotey et al. 2008b) were used to estimate the longwave properties of these materials.

Determination of Solar Heat Gain Coefficient

An energy balance on the window gives the net heat gain, Q_{net}, as the difference between the solar gain, Q_{solar}, and the heat loss, Q_{ht}, due to the temperature difference across the window, i.e.,

$$Q_{net} = Q_{solar} - Q_{ht} \tag{7}$$

By definition, Q_{solar} can be expressed as

$$Q_{solar} = SHGC_w \cdot G_{inc} \cdot A_w \tag{8a}$$

giving

$$SHGC_w = \frac{Q_{solar}}{A_w \cdot G_{inc}} \tag{8b}$$

where $SHGC_w$ is the solar heat gain coefficient of the window, A_w is the total projected window area and G_{inc} is the incident solar flux.

During testing, G_{inc} was measured with a pyranometer mounted on the mask wall while Q_{net} was measured based on

Table 5. Solar and Longwave Properties of Glazing and Shading Materials

Glazing/Shading Material	Normal Incidence Solar Properties				Longwave Properties	
	τ_{bt}	ρ_{bt}	τ_{bd}	τ_{bb}	ε	τ_{LW}
3 mm clear glass	0.83	0.08	0.00	0.83	0.84	0.00
Beige drapery fabric	0.24	0.55	0.22	0.02	0.89	0.06
Grey roller blind	0.13	0.29	0.02	0.11	0.80	0.17
Dark fiberglass insect screen	0.60	0.03	0.01	0.59	0.35	0.62
Venetian blind slat (black)	0.00	0.06	0.00	0.00	0.86	0.00
Venetian blind slat (white)	0.00	0.68	0.00	0.00	0.87	0.00

an energy balance over the control volume of the inner cell. The net energy flow through the window is comprised of energy absorbed by the absorber plate, Q_{abs}, heat loss through the calorimeter cell wall, Q_{cw}, heat loss due to air leakage, Q_{al} and electrical power inputs to the calorimeter, Q_{inp}.

$$Q_{net} = Q_{abs} + Q_{cw} + Q_{al} - Q_{inp} \quad (9)$$

All terms on the right hand side of Equation 9 are well defined in (CANMET 1993, Brunger et al. 1999) and were determined accordingly. Note that the more significant terms in Equation 9 are Q_{abs} and Q_{inp} since they are much greater than Q_{cw} and Q_{al}. Generally, the magnitudes of Q_{cw} and Q_{al} are such that they can be neglected.

By definition, Q_{ht} can be expressed as

$$Q_{ht} = U_w \cdot A_w \cdot \Delta T_w \quad (10)$$

where U_w is the overall window heat transfer coefficient and ΔT_w is the temperature difference across the window.

To obtain $SHGC_w$ from Equation 8, ΔT_w was maintained close to zero during the experiments (e.g., Harrison and van Wonderen 1994). This was achieved by holding the temperature within the calorimeter (indoor) and the environmental chamber (outdoor) at 20 ± 1°C (68 ± 1.8°F). Since zero temperature difference was not realised, the small temperature difference across the window was accounted for by estimating Q_{ht} and subsequently using the value of Q_{ht} to calculate Q_{solar}. See Equation 7. However, this adjustment was very small and influences the value of $SHGC_w$ typically in the third decimal place. A similar procedure has been used to obtain SHGC of windows with shading devices (Harrison and van Wonderen 1998 and Brunger et al. 1999).

In addition, the solar heat gain coefficient of the total glass area, $SHGC_g$ was obtained from $SHGC_w$ using an area-based calculation, i.e.,

$$SHGC_g = \frac{A_w}{A_g} SHGC_w \quad (11)$$

Equation 11 is based on the assumption that the solar heat gain coefficient of the frame, $SHGC_{fr}$ is negligible (Wright and McGowan 1999). The SHGC values reported in Table 6 are the values for $SHGC_g$.

The IAC, as defined by Equation 2, was subsequently obtained. The measured IAC values are also listed in Table 6. The uncertainty associated with the SHGC values was estimated to be ±0.03. Details of the uncertainty analysis of a typical SHGC measurement are documented in (CANMET 1993).

Determination of Solar Transmittance

The value of τ_{sys} was determined using Equation 12.

$$\tau_{sys} = \frac{G_{trans,1}}{G_{inc}} \quad (12)$$

Table 6. Summary of Measurement Results

Sample Description	SHGC	IAC	τ_{sys}
CDG window	0.73	1.00	0.67
CDG window + black insect screen	0.43	0.59	0.40
CDG window + beige pleated drape (100% fullness)	0.43	0.59	0.18
CDG window + white venetian blind (closed)	0.40	0.55	0.03
CDG window + white venetian blind (fully opened)	0.69	0.95	0.59
CDG window + white venetian blind (slat angle = 30^0)	0.63	0.86	0.38
CDG window + white venetian blind (slat angle = 60^0)	0.46	0.64	0.08
CDG window + grey roller blind	0.51	0.70	0.09
CDG window + black venetian blind (slat angle = 60^0)	0.67	0.92	0.02

where $G_{trans,1}$ is the indoor-side pyranometer reading adjusted for distance. The distance adjustment is necessary because the rays of incident radiation are not perfectly parallel. Therefore, the indoor-side pyranometer should have been mounted very close to the test sample at location 1. See Figure 1. However, it was mounted at location 2, a distance of 0.43 m (1.4 ft) from the indoor surface of the shading layer. At location 2, the pyranometer was able to view a representative area of the shading layer. Such an arrangement reduces the uncertainty in the transmittance measurements associated with non-homogeneous shading layers by eliminating the need to take several readings at different locations in the vertical plane. Nevertheless, the readings from the indoor-side pyranometer required adjustment to compensate for the decreased irradiance with distance.

Prior measurements of irradiance, G, with distance, D, from the solar simulator revealed an inverse power relation of the form

$$G = \text{constant}\left(\frac{1}{D}\right)^{1.83} \quad (13)$$

Given the irradiance at location 2, $G_{trans,2}$, the irradiance at location 1, $G_{trans,1}$ was calculated as

$$G_{trans,1} = G_{trans,2}\left(\frac{D_2}{D_1}\right)^{1.83} \quad (14)$$

where D_1 and D_2 are the distances from the solar simulator to locations 1 and 2, respectively. See Figure 1. The $G_{trans,1}$ value, as calculated from Equation 14 was subsequently substituted into Equation 12 to estimate τ_{sys}. The values of τ_{sys} are included in Table 6. The uncertainty associated with the measured τ_{sys} values was estimated to be ±0.03.

ASHWAT SIMULATION

The simulation entails a multi-layer analysis where each glazing/shading multi-layer system is treated as a series of parallel layers separated by gaps (Wright and Kotey 2006, Wright 2008). Solar-thermal separation is used to set up a two-step analysis. The first step involves the tracking of the incident solar radiation to determine the portions reflected, transmitted, and absorbed. The second step is an energy balance at each layer, accounting for heat transfer and the flux of absorbed solar radiation at each layer in order to obtain the set of layer temperatures and the corresponding heat flux values.

Solar Optical Analysis

In tracking the solar radiation as it interacts with glazing/shading layers an algorithm was devised to extend the solar-optical analysis of a system comprised of only specular glazing layers. This was necessary as a portion of incident beam solar radiation that encounters the shading layer will be scattered. The beam/diffuse characterization of solar radiation necessitates an expanded set of solar optical properties for each layer. Glazing layers are characterised by only specular properties while shading layers are characterized by a more extensive set of properties that describe the beam-beam, beam-diffuse and diffuse-diffuse actions of solar transmission and reflection. A small number of input values are required to describe any layer. These input properties are converted to the full set of layer properties by ASHWAT models (Wright et al. 2009). The ASHWAT models also make the adjustments necessary to account for off-normal and/or diffuse solar radiation (Kotey et al. 2008a, Kotey et al. 2009a, b, c, d). The solar optical analysis results include all beam and diffuse fluxes, providing full detail concerning the quantities of reflected, transmitted and absorbed radiation (Wright and Kotey 2006).

Heat Transfer Analysis

Having obtained the absorbed quantities from the solar-optical analysis, an energy balance is applied at each layer. The energy balance involves the formulation of radiative and convective exchange between the layers with absorbed solar radiation appearing as a source term. The resulting set of equations is solved for all layer temperatures and radiative and convective heat transfer rates. In turn it is possible to calculate indices of merit including U-factor and SHGC for any given environmental condition.

A technique for modeling the longwave radiant components of heat transfer is described in (Wright 2008). This technique, a net radiation formulation, is based on the radiant fluxes leaving the front and back surfaces of the each layer. The net radiant heat flux across a gap can be expressed as the difference between the radiosities of the bounding surfaces. The effective longwave properties of each layer are required as input. Details regarding the evaluation of these properties can be found in (Yahoda and Wright 2004, Kotey et al. 2008b and Wright et al. 2009).

The quantification of convective components of heat transfer relies largely on empirical information. Methods to obtain convective heat transfer coefficients for glazing cavities are well established (e.g., Elsherbiny et al 1982, Wright 1996, Shewen et al 1996). On the other hand, the convective heat transfer coefficients used at the exposed surfaces are specified by the calling routine (i.e., the building simulation or performance rating program). Values may be specified to differentiate between natural and forced convection. Established values are available in the limiting cases where the shading layer is spaced well away from the window or where the spacing approaches zero. Knowing these limits, a model has been formulated to make a smooth transition so the user can place the shading layer at any distance from the surface of the window. This model is documented in (Wright et al. 2009).

Simulation Results

The same test conditions summarised in Table 1 were used as input to the current version of the ASHRAE toolkit that incorporates the ASHWAT models. The mean radiant temperatures were assumed to be equal to the air temperatures. Solar, longwave and geometric properties of the individual layers including the distance between glazing/shading layers were also supplied to the simulation program.

A wide variety of output parameters such as layer temperature, heat flux values, absorbed solar radiation, τ_{sys}, $SHGC_{cg}$, IAC and U-value could be extracted from the simulation. However, for the current investigation, only τ_{sys}, $SHGC_{cg}$, IAC and U-factor were obtained. See Table 7. Note that the value of $SHGC_{cg}$ is routinely equated to $SHGC_g$. Thus the SHGC values listed in Table 7 are those of $SHGC_g$. The U-factors listed in Table 6 are the centre glass U-factors, i.e., U_{cg}. The window U-factor, U_w, was required to make a small adjustment in determining the measured $SHGC_w$. See Equations 7, 8 and 10. However, for a large window having a smaller edge glass and frame area fractions, U_{cg} is approximately equal to U_w, and this approximation was used.

DISCUSSION

Effect of Shading Devices on Solar Gain

The measurement and simulation results are summarised in Tables 6 and 7, respectively. In each case the shading device reduces solar gain; SHGC values for the shaded window are lower than the corresponding value for the unshaded window. The reduction in solar gain by shading devices is also evident from IAC values with lower IAC values corresponding to greater reduction in solar gain.

The white venetian blind in the closed position gives the largest reduction in solar gain. This can be attributed to high solar reflectance of the white slats. Higher solar reflectance will result in greater rejection of insolation. Furthermore, there is complete blockage of beam insolation by the closed slats. Thus, amongst the indoor shading devices considered, the white venetian blind has the greatest potential to reduce

Table 7. Summary of Simulation Results

Sample Description	SHGC	IAC	τ_{sys}	U-factor, W/m^2·K (Btu/hr·ft·°F)
CDG window	0.76	1.00	0.69	2.76 (0.49)
CDG window + black insect screen	0.47	0.61	0.42	2.77 (0.49)
CDG window + beige pleated drape (100% fullness)	0.49	0.65	0.17	2.49 (0.44)
CDG window + white venetian blind (closed)	0.43	0.56	0.05	2.49 (0.44)
CDG window + white venetian blind (fully opened)	0.74	0.97	0.63	2.63 (0.46)
CDG window + white venetian blind (slat angle = 30^0)	0.64	0.83	0.35	2.62 (0.46)
CDG window + white venetian blind (slat angle = 60^0)	0.49	0.64	0.10	2.54 (0.45)
CDG window + grey roller blind	0.58	0.76	0.10	2.56 (0.45)
CDG window + black venetian blind (slat angle = 60^0)	0.68	0.90	0.00	2.54 (0.45)

cooling loads. On the other hand, the lowest reduction in solar gain was achieved when the white venetian blind was fully opened. This is because in the fully opened position the slats are aligned with the beam and intercept only a small portion of the insolation. The partially opened white blind (slat angle = 30°, 60°) gives IAC values in between those of the fully opened and closed positions with the 30° slat position recording a higher IAC than the 60° slat position. This is due to the fact that the 60° slat position blocks more beam insolation as compared to the 30° slat position. The variation in IAC demonstrated by these results attests to the suitability of venetian blinds as operable solar control devices.

Considering the black venetian blind with slat angle = 60°, it is interesting to note a fairly low reduction in solar gain compared to the white venetian blind with the same slat angle. This observation is primarily due to a much lower reflectance of black slats compared to white slats. In addition, the black blind absorbs more solar energy than the white blind. Given that both blinds are located at the indoor side of the window, a much higher flux of absorbed energy is redirected to the indoor side by heat transfer from the black blind.

Another interesting observation is that the indoor mounted pleated drape has about the same effect as the outdoor mounted insect screen. Table 5 reveals that the insect screen has a much higher solar transmittance compared to the drape fabric. On the other hand, the drape fabric has a higher solar reflectance. Note that the drape in its pleated form will have slightly lower effective solar reflectance and transmittance values in comparison with the fabric from which it is made (Kotey et al 2009d). The insect screen might be expected to deliver more solar gain since it has a higher solar transmittance and a much lower solar reflectance. However, because the screen was located on the outdoor side, the absorbed solar energy was mostly dissipated to the outdoor air.

Also, it is worth mentioning that the potential for any given shading device to control solar gain (i.e., its IAC) is influenced by the glazing system to which it is attached. Consider two categories of glazing systems.

1. High-SHGC: A simple glazing system consisting of one or two layers of clear glass will produce high solar gain. The solar gain will consist almost entirely of transmitted solar radiation and this is evident because the solar transmittance of the glazing system will be only slightly less than its SHGC value (i.e., the ratio $\tau_{sys}/SHGC$ will be high, close to unity).
2. Low-SHGC: A more sophisticated glazing system that includes tinted glass and/or one or more coatings will generally produce low solar gain. In this case less of the solar gain will consist of transmitted solar radiation. A large portion of the solar gain will result from absorbed solar radiation that makes its way to the indoor space by means of heat transfer. The solar transmittance of the glazing system will be much less than its SHGC value (i.e., the ratio $\tau_{sys}/SHGC$ will be low, closer to zero).

If a glazing system is in the high-SHGC category the solar gain can be controlled effectively using an indoor attachment with high solar reflectance. It is widely acknowledged that solar reflectance is the most important performance characteristic of a shading device. The challenge of controlling solar gain is largely a matter of solar optics in this case and this is demonstrated in the comparison between white and black venetian blinds.

In contrast, if the glazing system is in the low-SHGC category the solar reflectance of an indoor attachment will have little influence because most of the solar gain arrives by means of heat transfer. In addition, examining the U-values listed in Table 7, it can be seen that the shading attachments have very little influence on thermal resistance. Therefore, indoor shading attachments offer little potential for controlling the solar gain produced by low-SHGC glazing systems. However, the solar gain of any glazing system can be controlled by locating the shading device on the outdoor side of the building. This arrangement allows the solar radiation to be intercepted, either absorbed or reflected, before it can be absorbed or transmitted by the glazing system. This point

is demonstrated by the comparison between the pleated drape and the outdoor insect screen.

Comparison between Measurement and Simulation Results

The comparison of NSTF measurements and ASHWAT simulation results is shown graphically in Figures 3 through 6.

Figure 3 shows very good agreement between NSTF measurements of solar transmission and the ASHWAT models. With an average difference of 0.02 and a maximum difference of 0.04 there is remarkably good agreement between the two sets of results. The discrepancy, expressed as a percentage, is appreciable only for systems with very low solar transmission. With the exception of the fully opened white venetian blind, the difference between the measurement and simulation results is well within measurement uncertainty.

The comparison of measured versus calculated SHGC is shown in Figure 4. The average difference between the two sets is 0.04. In most cases, the difference is within measurement uncertainty. The white venetian blind (slat angle = 30°) and black venetian blind (slat angle = 60°) give the best agreement while the roller blind shows a difference of 0.07. Again, there is good agreement but the calculated SHGC is consistently greater than the measured SHGC. As a result of this observation some additional investigation was undertaken.

Noting that there is no bias in the solar transmission data, Figure 3, it was concluded that the bias seen in Figure 4 must be caused by some aspect of the heat transfer process. The most likely cause is the assignment of convective heat transfer coefficients for surfaces exposed to the environment. The indoor and outdoor convection heat transfer coefficients used to produce Figure 4 were $h_{c,in}$ = 4.6 W/m2·K (0.8 Btu/ft^2·h·°F) and $h_{c,out}$ = 10.1 W/m^2·K (1.8 Btu/ft^2·h·°F). In order to test the sensitivity of SHGC with respect to these coefficients the simulations were re-run with heat transfer coefficients more typical of the ASHRAE summer design condition, $h_{c,in}$ = 4.0 W/m2·K (0.7 Btu/ft^2·h·°F) and $h_{c,out}$ = 15.0 W/m^2·K (2.6 Btu/ft^2·h·°F), and again the calculated results were compared against NSTF measurements. See Figure 5. In the new comparison the agreement between ASHWAT and NSTF results has improved with an average difference of only 0.02 and the bias is gone. The white venetian blind gives a perfect correlation both in the closed and slat angle = 60° position while the pleated drape records a maximum difference of 0.04. The point of this exercise is not necessarily to assert that the heat transfer coefficients supplied for the NSTF facility are wrong. It is more informative to note that the uncertainties attached to the total heat transfer coefficients are large (recall

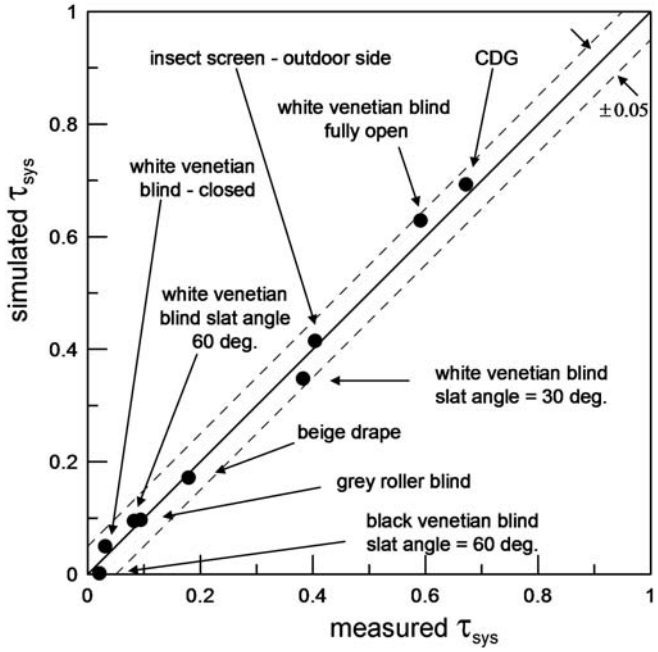

Figure 3 *Comparison of centre-glass τ_{sys} values, simulation versus measurements, normal incidence, various shading layers attached to CDG window.*

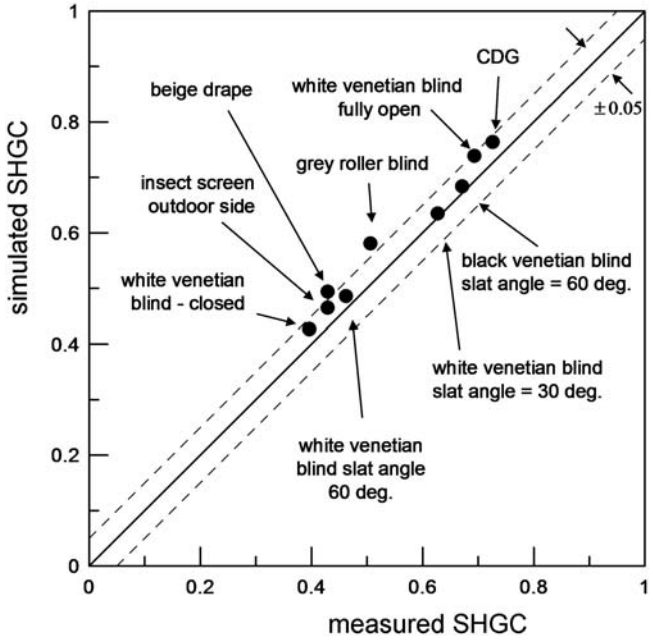

Figure 4 *Comparison of centre-glass SHGC values, simulation versus measurements, normal incidence, various shading layers attached to CDG window, $h_{c,in}$ = 4.6 W/m^2·K (0.8 Btu/ft^2·h·°F) and $h_{c,out}$ = 10.1 W/m^2·K (1.8 Btu/ft^2·h·°F).*

$h_{tot,in}$ = 9.6 ±1.9 W/m^2·K [1.7 ± 0.3 Btu/ft^2·h·°F] and $h_{tot,out}$ = 16.5 ± 5.3 W/m^2·K [2.9 ± 0.9 Btu/ft^2·h·°F]). This is primarily because the CTS was not calibrated (van Wonderen 1995). The modified heat transfer coefficients used to produce Figure 5 actually fall within the range of those uncertainties. The modified comparison simply highlights the idea that SHGC is mildly sensitive to the surface convective heat transfer coefficients and that this might be a suitable topic for future research if higher accuracy is desired.

Finally, measured and calculated IAC values were compared and the ASHWAT/NSTF comparison is shown in Figure 6. Again the agreement is very good. The average difference between the two sets of results is 0.03 and a maximum difference of 0.06 is observed for the pleated drape and the roller blind. Note that regardless of whether the SHGC data shown in Figure 4 or Figure 5 are used, the resulting values of calculated IAC and Figure 6 are virtually unchanged. In other words, although some sensitivity in SHGC has been demonstrated, the sensitivity of IAC with respect to the surface convection coefficients is weak. There are several reasons for this insensitivity including the ideas that (a) the solar transmission is unaffected by convection and (b) changes in convective heat transfer will influence the shaded and unshaded windows in a similar fashion – causing a similar increase or decrease in the SHGC of both.

On a more general note, the uncertainty associated with the measured values of SHGC was estimated to be ±0.03. Small differences between the measured and simulated SHGC values may also be attributed to uncertainty in the measured input values used in the simulation. For example, the solar properties obtained from the spectrophotometer (Kotey et al. 2009a, b and c) have an uncertainty of ±0.03. Furthermore, minor differences in the SHGC values may also be attributed to the approximations in the ASHWAT models in particular the convection models associated with open-channel attachment. However, it is difficult to pinpoint sources of discrepancy because the agreement is very good.

In summary, very good agreement between the measured and the simulated solar gain is clearly demonstrated in Figures 3, 4, 5 and 6 since the absolute difference in almost all cases is within 0.05.

CONCLUSION

A comparison between measured and simulated solar gain in windows with shading devices is reported. The measurements were taken using the NSTF solar simulator and solar calorimeter. The shading devices investigated include

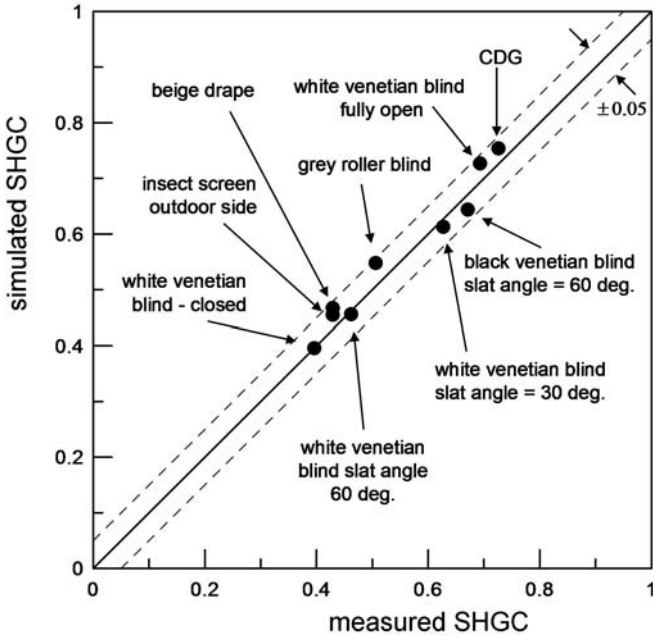

Figure 5 *Comparison of recalculated and measured centre-glass SHGC values, normal incidence, various shading layers attached to CDG window,* $h_{c,in}$ = 4.0 W/m^2·K (0.7 Btu/ft^2·h·°F) and $h_{c,out}$ = 15.0 W/m^2·K (2.6 Btu/ft^2·h·°F).

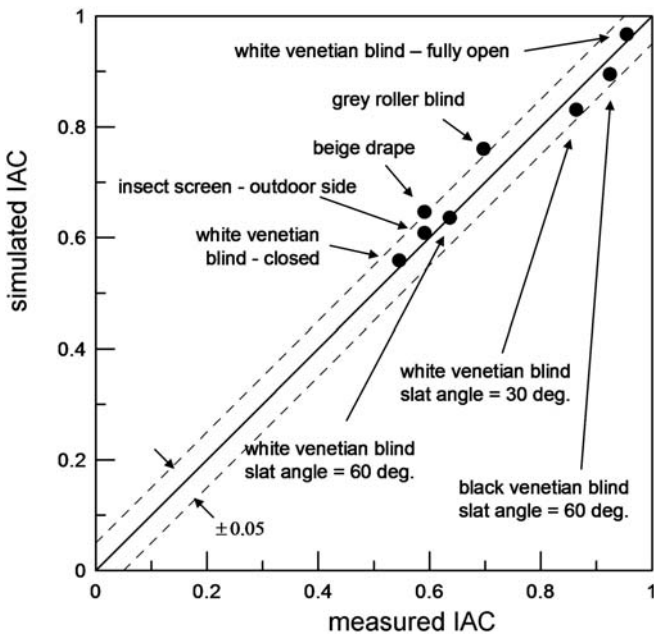

Figure 6 *Comparison of centre-glass IAC values, simulation versus measurements, normal incidence, various shading layers attached to CDG window.*

two venetian blinds, a roller blind, a pleated drape and an insect screen. The calculations were obtained from a comprehensive fenestration/shading model, designated ASHWAT which was developed for building energy simulation and performance rating. In general, there is very good agreement between the measured and simulated values of SHGC, IAC and τ_{sys}. In most cases the discrepancy between measurement and simulation is well below 0.05. The differences between the two sets offer little insight regarding shortcomings of either technique because the agreement is very good. However, the current study provides insight regarding the effect of different types of shading devices, their colour and their location on the solar gain in windows as well as confidence in the simulation and measurement procedures used. Nonetheless, this exercise should be viewed as a useful step at an early stage in the development of shading system analysis tools. Several opportunities for future research are evident. Suggestions include measurements using a wider variety of shading attachments and glazing systems, more accurate CTS experiments to better evaluate surface convection coefficients, measurements designed to examine the effect of glazing/shading layer spacing and measurements over a range of larger off-normal incidence angles. These and other experiments will make it possible to further validate and fine tune the simulation models.

ACKNOWLEDGMENTS

We would like to thank NRCan (Natural Resources Canada), NSERC (Natural Scienes and Engineering Research Council Canada) and ASHRAE for financial support. We would also like to thank Alfred Brunger and Larry West of the NSTF for their contributions. Special thanks to Corey Lindner of Golden Windows Ltd. (Kitchener, ON) for supplying the IGU.

REFERENCES

ASHRAE. 2005. *ASHRAE Handbook-Fundamentals*. Atlanta: American Society of Heating Refrigeration and Air Conditioning Engineers, Inc.

ASTM E891-87. 1987. *Standard Tables for Terrestrial Direct Normal Solar Spectral Irradiance for Air Mass 1.5*. Philadelphia: American Society for Testing and Materials.

ASTM E903-96. 1996. *Standard Test Method for Solar Absorptance, Reflectance, and Transmittance of Materials Using Integrating Spheres*. Philadelphia: American Society for Testing and Materials.

Barnaby, C. S., J. D. Spitler, and D. Xiao. 2004. Updating the ASHRAE/ACCA residential heating and cooling load calculation procedures and data. RP-1199 final report. ASHRAE.

Barnaby, C.S., Wright, J.L., Collins, M.R. 2009. Improving load calculations for fenestration with shading devices. ASHRAE Transactions 115(2).

Brunger, A., Dubrous, F.M., and S.J. Harrison. 1999. Measurement of the solar heat gain coefficient and u-value of windows with insect screens. ASHRAE Transactions, 105(2): 1038-1044.

CANMET. 1993. The determination of fenestration solar heat gain coefficient using simulated solar irradiance. Report prepared for Natural Resources, Canada. The Solar Calorimetry Laboratory, Queen's University, Kingston, Ontario.

CSA. 1998. CSA Standard A440.2-98. Energy performance of windows and other fenestration systems. Toronto: Canadian Standard Association.

EEL, 1995. FRAMEplus toolkit: A Comprehensive Tool for Modelling Heat Transfer in Windows, Doors, Walls and Other Building Components. Enermodal Engineering Ltd., Waterloo, Ontario.

ElSherbiny, S.M., Raithby, G.D. and Hollands, K.G.T. 1982. Heat transfer by natural convection across vertical and inclined air layers, Journal of Heat Transfer, 104: 96-102.

EnergyPlus. 2007. *EnergyPlus Engineering Reference – The Reference to EnergyPlus Calculations*, U.S. Department of Energy.

Farber, E.A., Smith, W.A., Pennington, C.W., and J.C. Reed. 1963. Theoretical analysis of solar heat gain through insulating glass with inside shading. ASHRAE Journal, pp. 79.

Harrison, S.J., and F Dubrous. 1990. Determination of Window Thermal Characteristics Using a Solar Simulator Based Test Method. ASHRAE Transactions, 96(1): 912-919.

Harrison, S.J., and S.J. van Wonderen. 1994. Determining window solar heat gain coefficient. ASHRAE Journal, 36(8): 26-32.

Harrison, S.J., and S.J. van Wonderen. 1998. Evaluation of solar heat gain coefficient for solar-control glazings and shading devices. ASHRAE Transactions, 104(1).

Hellstrom, B., Kvist, K., Hakansson, H., and H. Bulow-Hube. 2007. Description of ParaSol v3.0 and comparison with measurements. Energy and Buildings 39: 279-283.

Hollands K.G.T., Wright, J. L. and Granqvist, C., 2001. Chapter 2: Glazings and Coatings, in Gordon, J.M. Solar Energy: a Century of Progress. James and James, London, U.K. 29-107.

Huang, N.Y.T., Wright, J.L. and Collins, M.R. 2006. Thermal Resistance of a Window with an Enclosed Venetian Blind: Guarded Heater Plate Measurements. ASHRAE Transactions, 112 (2): 13-21.

ISO, 2004. Windows and Doors, Thermal Transmission Properties - Detailed Calculation. ISO Final Draft Standard 15099.

Kotey, N.A., Collins, M.R., Wright, J.L., and T. Jiang. 2008a. A simplified method for calculating the effective solar optical properties of a venetian blind layer for building energy simulation. ASME Journal of Solar Energy Engineering, 131(2).

Kotey, N.A., Wright, J.L. and M.R. Collins. 2008b. Determining Longwave radiative properties of flat shading materials. SESCI 2008, Fredericton, New Brunswick.

Kotey, N.A., Wright, J.L. and M.R. Collins. 2009a. Determining off-normal solar optical properties of drapery fabrics. ASHRAE Transactions, 115(2).

Kotey, N.A., Wright, J.L. and M.R. Collins. 2009b. Determining off-normal solar optical properties of roller blinds. ASHRAE Transactions, 115(1).

Kotey, N.A., Wright, J.L. and M.R. Collins. 2009c. Determining off-normal solar optical properties of insect screens. ASHRAE Transactions, 115(1).

Kotey, N.A., Wright, J.L. and M.R. Collins. 2009d. A detailed model to determine the effective solar optical properties of draperies. ASHRAE Transactions, 115(1).

Mitchell R., Kohler C, Klems J, Rubin M, and D. Arasteh. 2006. WINDOW 6.1/THERM 6.1Reserach Version User Manual, Environmental Energy Technologies Division, Lawrence Berkeley Laboratory, Berkeley, California.

Parmelee, G. V. and W.W. Aubele.1952. The shading of sunlit glass: an analysis of the effect of uniformly spaced flat opaque slats. ASHVE Transactions 58: 377-398.

Pedersen, C. O., R. J. Liesen, R. K. Strand, and D. E. Fisher. 2001. *Toolkit for building load calculations*. Atlanta: American Society of Heating Refrigeration and Air Conditioning Engineers, Inc.

Pfrommer, P., Lomas, K.J., and Chr. Kupke.1996. Solar radiation transport through slat-type blinds: A new model and its application for thermal simulation of buildings. Solar Energy. 57(2): 77-91.

Rheault, S. and Bilgen, E., 1989. Heat Transfer Analysis in an Automated Venetian Blind System. ASME Journal of Solar Energy Engineering. 111: 89-95.

Rosenfeld, J.L.J., Platzer, W.J., Van Dijk, H., and Maccari, A. 2000. Modelling the Optical and Thermal Properties of Complex Glazing: Overview of Recent Developments. Solar Energy, Vol. 69 Supplement, No. 1-6, pp.1-13.

Rubin, M. 1982. Calculating heat transfer through windows, Energy Research, 6: 341-349.

Shewen, E., Hollands, K.G.T., Raithby, G.D. 1996. Heat Transfer by Natural Convection Across a Vertical Cavity of Large Aspect Ratio. Journal of Heat Transfer, 118: 993-995.

van Dijk, H., Kenny, P., and J. Goulding. (eds), 2002. WIS – Advanced Windows Information System – Reference Manual.

van Wonderen, S. Experimental Determination of Fenestration Solar Heat Gain Coefficient, MASc Thesis. 1995. Queens University. Kingston. Ontario.

Wright, J.L. 1986. Effective U-values and Shading Coefficients of Preheat/Supply Air Glazing Systems. Proc. Solar Energy Society of Canada, Winnipeg. 219-224.

Wright, J.L. 1995a. Summary and Comparison of Methods to Calculate Solar Heat Gain. ASHRAE Transactions, Vol 101(1): 802-818.

Wright, J.L. 1995b. VISION4 Glazing System Thermal Analysis: Reference Manual. Advanced Glazing System Laboratory, University of Waterloo.

Wright, J.L. 1996. A Correlation to Quantify Convective Heat Transfer Between Vertical Window Glazings. ASHRAE Transactions, 102(1): 940-946.

Wright, J.L., and A. McGowan. 1999. Calculating solar heat gain of window frames. ASHRAE Transactions, 105(2): 1011-21.

Wright, J.L., and N.A. Kotey. 2006. Solar absorption by each element in a glazing/shading layer array. ASHRAE Transactions, 112(2): 3-12.

Wright, J.L., 2008. Calculating Centre-Glass Performance Indices of Glazing Systems with Shading Devices. ASHRAE Transactions, 114(2).

Wright, J.L., Huang, N.Y.T., Collins, M.R. 2008. Thermal Resistance of a Window with an Enclosed Venetian Blind: A Simplified Model. ASHRAE Transactions, 114(1).

Wright, J.L., Barnaby, C.S., Collins, M.R. and Kotey, N.A. 2009. Improving Cooling Load Calculations for Fenestration with Shading Devices, Final Report, ASHRAE Research Project 1311.

Yahoda, D.S. and J.L. Wright, J.L. 2004. Methods for Calculating the Effective Longwave Radiative Properties of a Venetian Blind Layer. ASHRAE Transactions, 110(1): 463-473.

Yahoda, D.S. and J.L. Wright. 2005. Methods for calculating the effective solar-optical properties of a venetian blind layer. ASHRAE Transactions, 111(1): 572-586.